Large-scale seroepidemiology uncovers nephro-urological pathologies in persons with tau autoimmunity

Authors:

Andreia D. Magalhães[1†], Marc Emmenegger[1&], Elena De Cecco[1], Manfredi Carta[1‡], Karl Frontzek[1], Andra Chincisan[1||], Jingjing Guo[1], Simone Hornemann[1*], Adriano Aguzzi[1*]

Affiliations:

[1]Institute of Neuropathology, University of Zurich; CH-8091 Zurich, Switzerland

[†] Present address: Department of Neurology, Inselspital, Bern University Hospital; CH-3010 Bern, Switzerland

[&]Present address: Division of Medical Immunology, Department of Laboratory Medicine, University Hospital Basel; CH-4031 Basel, Switzerland

[‡]Present address: Institute of Neurology, University of Zurich; CH-8091 Zurich, Switzerland

§ Present address: University College London, Institute of Neurology, Queen Square Brain Bank; WC1N 1PJ London, United Kingdom

[||] Present address: Credit Suisse; CH-8001 Zurich, Switzerland

[*]Correspondence: Simone Hornemann and Adriano Aguzzi

Institute of Neuropathology, University of Zurich; CH-8091 Zurich, Switzerland

Phone: 0041 44 255 2107

Simone.hornemann@uzh.ch and adriano.aguzzi@uzh.ch

Competing interests:

AA is a member of the Board of Directors of Mabylon AG. Mabylon AG produces therapeutic human antibodies. Mabylon AG had no insight and no influence on the current study. All authors report no other relationships or activities that could appear to have influenced the submitted work.

Abstract:

Intraneuronal aggregates of the microtubule-associated protein tau play a pivotal role in Alzheimer's disease and several other neurodegenerative syndromes. Anti-tau antibodies can reduce pathology in mouse models of neurodegeneration and are currently being tested in humans. Here, we performed a large-scale seroepidemiological search for anti-tau IgG autoantibodies (ατ) on 40,497 human plasma samples. High-titer $\alpha\tau^+$ individuals were surprisingly prevalent, with hospital patients being three times more likely to be $\alpha\tau^+$ ($EC_{50} \geq 2^6$, corresponding to a nominal dilution of > 1/64) than healthy blood donors (4.8% vs 1.6%), The prevalence increased with age higher than 70 years-old (RR 1.26, 95%CI 1.11-1.43, P<0.001) and was higher for women (RR 1.20, 95%CI 1.07-1.39, P=0.002). The autoantibodies bound selectively to tau, inhibited tau aggregation *in vitro*, and interfered with tau detection in plasma samples. No association was found between ατ autoantibodies and neurological disorders. Instead, tau autoreactivity showed a significant association with kidney and urinary disorders (adjusted RR 1.27, 95% CI 1.10-1.45, P=0.001 and 1.40, 95% CI 1.20-1.63, P<0.001, respectively). These results suggest a previously unrecognized association between ατ autoimmunity and extraneural diseases.

Main Text:

INTRODUCTION

Tau is a microtubule binding protein involved in cytoskeletal dynamics and expressed in neurons (1, 2) and in extraneural tissues, including kindey (1-5). It plays a pivotal role in a variety of neurodegenerative diseases, including Alzheimer's disease (AD) (6), progressive supranuclear palsy, and various syndromes collectively referred to as tauopathies (7). The presence of brain neurofibrillary tau tangles correlates with cognitive decline (8), and plasma measurements of total and phosphorylated tau have emerged as promising biomarkers for the detection and monitoring of AD progression (9-12). Moreover, active and passive immunization with antibodies against a wide range of tau epitopes can reduce pathology and functional decline in animal models of tauopathies (13, 14) and are being tested in clinical trials of neurodegenerative diseases (15).

Natural autoantibodies are immunoglobulins generated against self-antigens in the absence of external antigen stimulation (16). They are a normal part of the immunoglobulin repertoire and have physiological roles in homeostasis and surveillance, including the clearance of cellular debris, anti-inflammatory activity, and first-line defense against pathogens (17). However, in certain situations, natural autoantibodies can also cause pathological autoimmunity. The study of natural autoantibodies can therefore inform about properties of their targets, e.g. unrecognized protective or contributing roles in disease (18). Some natural autoantibodies can cause neurological disorders, such as antibodies targeting the N-methyl-D-aspartate receptor (NMDAR) in encephalitis (19) or antibodies targeting aquaporin-4 (AQP4) in neuromyelitis optica (20). Conversely, natural antibodies against amyloid-β have been suggested to protect and slow the progression of AD; aducanumab, a monoclonal antibody developed from B-cells of cognitively normal older age individuals, has been studied as a treatment for AD (21).

Anti-tau autoantibodies have been detected in plasma of patients with AD (22) and Parkinson's disease (23), but also in non-neurodegeneration controls (22). The effects, if any, of natural anti-tau autoantibodies in modulating the risk of developing neurodegenerative diseases are unknown. The study of individuals with anti-tau autoantibodies could clarify their potential as modifiers or biomarkers of disease. Here, we tested 40,497 plasma samples from healthy blood donors and from patients admitted to a university hospital in the frame of a two-sites cross-sectional study. We found that anti-tau autoimmunity is highly specific and surprisingly frequent, with its prevalence increasing with age. Unexpectedly, natural anti-tau autoantibodies were associated with a previously unrecognized syndrome comprising kidney and urinary disorders.

RESULTS

Prevalence of naturally occurring plasma anti-tau autoantibodies

We designed a cross-sectional study to investigate naturally occurring plasma IgG autoantibodies against MTBD-tau. Plasma samples from 32,291 university hospital patients (age ≥ 18 years) and 8,206 healthy blood donors were screened by miniaturized ELISA (Figure 1A) (24-26).

We excluded 7,952 and 1,616 non-informative samples from patients and blood donors, respectively (fitting error >20% $-\log_{10}(EC_{50})$ or high background), and analyzed 24,339 patient samples and 6,590 healthy blood-donor samples (Figure 1A). A titer of $-\log_{10}(EC_{50}) \geq 1.8$, approximately corresponding to a nominal dilution of > 1/64, was selected as a cutoff to call tau-autoreactive samples (henceforth named $\alpha\tau^+$). 1,169 hospital samples (4.80%) but only 104 healthy donor samples (1.58%) were $\alpha\tau^+$ (Figure 1A-C). Hence, anti-tau immunoreactivity was more prevalent in unselected hospital patients than in healthy individuals (P<0.001). Demographic data was available for 4,157 of the 6,590 blood donors. Median ages were 42 (IQR 29-54) and 55 years (IQR: 40-69) for healthy donors and hospital patients, respectively (P<0.001). Of the healthy blood donors, 40.9% (n=1,698) were women, whereas for the hospital group, 47.7% (n=11,609) of the patients were women (P<0.001). Multivariate log-binomial regression (27, 28) adjusted for age and sex showed that hospital patients had a 2.3x higher risk than healthy donors to be $\alpha\tau^+$ (aRR 2.30, 95%CI 1.83-2.92, P<0.001, Figure 1D).

The replicability of the microELISA screen was found to be high (R^2=0.84, P<0.001, Figure 1E). There was no cross-reactivity to two other proteins implicated in neurodegeneration, amyloid-ß pyroglutamate and the cellular prion protein (PrP^C) (26). Of 12,297 patient samples, 604 samples were positive against MTBD-tau and 5 against amyloid-ß pyroglutamate but none was cross-reactive against both targets (P=1, χ^2 test) (Figure 1F), Moreover, of 13,099 patient samples, 694 were

reactive against MTBD-tau and 15 against PrP^C, but again none was cross-reactive against both targets (P=0.734, χ^2 test) (Figure 1G).

Specificity and biological activity of $\alpha\tau^+$ samples

To investigate their specificity, we purified anti-tau autoantibodies by MTBD-tau affinity chromatography from four individual $\alpha\tau^+$ patients (P1-P4) and from a pool of six $\alpha\tau^+$ sample (patient_IDs: J909190817, J802220975, J909190382, J90806029, J908060881 and J805040458). Purified anti-MTBD-tau autoantibody samples had EC_{50} values of 0.042-14.45 µg/ml whereas the mouse anti-MTBD-tau antibody RD4 (29) had EC_{50}=0.002 µg/ml (Figure 2A). In a soluble-competition immunoassay (Figure 2B), purified $\alpha\tau^+$ autoantibodies showed a concentration-dependent binding to recombinant MTBD-tau purified by cation exchange and size exclusion chromatography and to a pool of 8 synthetic MTBD-tau peptides but not to albumin or an unrelated synthetic peptide (Figure 2C). To probe for polyreactivity, purified $\alpha\tau^+$ autoantibodies were tested against several structurally unrelated autoantigens and bacterial proteins, including MTBD-tau, albumin, cardiolipin, DNA, insulin, and lipopolysaccharides (LPS). Anti-tau autoantibodies were reactive against MTBD-tau but not against any of the other antigens or uncoated plates (Figure 2D).

In immunofluorescent stainings, purified $\alpha\tau$ autoantibodies co-localized to cytoplasmic EGFP-0N4RTau in SH-SY5Y cells and showed similar binding patterns to an anti-tau mouse monoclonal antibody H7, but not to non-transfected cells (Figure 2E). On western blots, purified $\alpha\tau$ autoantibodies detected tau-specific bands in cell lysates of SH-SY5Y cells overexpressing $tau^{P301L/S320F}$, but not in parental (wt) SH-SY5Y cells (Figure 2F and Supplemental Figure 1). Hence, the immunoreactivity of $\alpha\tau^+$ samples was highly specific for tau. All IgG subclasses and both κ and λ light

chains were present in $\alpha\tau^+$ patients' samples (Figure 2G and H). Epitope mapping and light-chain typing revealed a polytypic response for 23% of the $\alpha\tau^+$ samples (Figure 2H and I).

To investigate whether purified $\alpha\tau^+$ autoantibodies interfere with the aggregation of MTBD-tau, samples from patients P7 and P8 were tested in an *in vitro* tau aggregation assay (30). MTBD-tau aggregation was induced by heparin and shaking and monitored using Thioflavin T (ThT; Figure 3A). The presence of $\alpha\tau^+$ autoantibodies reduced the plateau of the ThT fluorescence signal in the kinetic trace by about half, whereas antibodies purified by protein G affinity chromatography from an $\alpha\tau^-$ patient had no effect (Figure 3A). Hence, $\alpha\tau^+$ autoantibodies inhibit MTBD-tau aggregation *in vitro*.

Plasma tau is a promising biomarker of progression for several neurological diseases (9-12, 31). We examined the effects of $\alpha\tau$ autoantibodies onto the performance of plasma tau immunoassays (Figure 3B). Purified $\alpha\tau$ autoantibodies from 5 patients (P2-P6) were added to tau^{441}-spiked plasma. After incubation, the amount of free tau^{441} was analyzed by ELISA using commercial anti-tau antibodies for capture (BT2, epitope on human tau^{441}: residues 194-198) and detection (ab64193, epitope on non-phosphorylated and phosphorylated human tau^{441} surrounding residue 262) (32). Purified $\alpha\tau$ autoantibodies P4-P6 induced a concentration-dependent impairment of detection of tau^{441} hampering the detection of plasma-spiked tau^{441} by approximately tenfold at higher anti-MTBD-tau autoantibody concentration (Figure 3C and D). In contrast, P2-P3 did not show any significant impairment of the detection of plasma-spiked tau^{441}. This variability of interference is explained by the binding epitopes on tau^{441}. P4-P6 occupy tau residues 244 to 282 including the binding epitope of ab64193, whereas P2-P3 occupy residues 273 to 327 which are outside the epitope of ab64193 (Figure 3C and D and Supplemental Figure 2). Hence, the presence of $\alpha\tau^+$ autoantibodies can interfere with the detection of plasma tau in immunoassays depending

on the combination of epitopes of the patient samples and of commercial antibodies used in immunoassays.

Demographic characteristics of tau-immunoreactive patients

The age of $\alpha\tau^+$ patients (median: 58 years; IQR: 43-71) was significantly higher than that of $\alpha\tau^-$ (median: 55; IQR: 40-68; $P < 0.001$, Figure 4A). Univariate logistic regression analyses of health records for the 24,339 hospital patients showed that the prevalence of $\alpha\tau$ immunoreactivity increased with age, from 3.9% in patients aged <29 years to 7.6% in patients aged >90 years ($P<0.001$, Figure 4B). A log-binomial regression model (27, 28) estimated that the RR for the presence of anti-MTBD-tau autoantibodies was highest for patients aged 70-99 years (RR 1.26, 95% CI 1.11-1.43, $P<0.001$, Figure 4C) and for women (RR 1.20, 95% CI 1.07-1.39, $P=0.002$, Figure 4C). Due to the association of anti-MTBD-tau autoantibodies with increased age and female sex, all further RRs were calculated using a multivariate log-binomial regression model adjusted for age and sex. To identify potential correlations between $\alpha\tau^+$ and specific diseases, we analyzed the admission to clinical departments. The highest RRs for $\alpha\tau^+$ were found for angiology (aRR 1.84, 95% CI 1.21-2.63, $P=0.002$) and nephrology (aRR 1.50, 95% CI 1.16-1.89, $P=0.001$, Figure 4D-E), whereas no significant difference was found between the percentage of $\alpha\tau^+$ and $\alpha\tau^-$ patients from the department of neurology (Figure 4D).

Neurological disorders and anti-tau autoimmunity

We next mined pseudonymized clinical diagnoses from the clinical records of the USZ pertaining to the diagnoses of 23,375 patients as represented by ICD-10 codes (Figure 5A). Given the in-

volvement of tau in neurodegenerative diseases (6), we focused on evaluating the association between anti-MTBD-tau autoantibodies and neurological diseases, which we categorized in 23 main groups of disorders. No associations between $\alpha\tau^+$ and neurological diseases were identified (Figure 5A). We further performed a targeted screen using plasma samples from 47 patients with AD and 68 similarly aged non-AD patients selected from our plasma biobank (median age of AD patients 78 years, IQR 70,5-86, and median age of control patients 81 years, IQR 71-85, Supplemental Table 1). Samples were tested for anti-MTBD-tau IgG autoantibodies, as in the primary screen, and additionally for anti-MTBD-tau IgA autoantibodies and anti-full-length-tau IgG and IgA autoantibodies. No significant difference in reactivity was observed between the plasma samples from AD patients and non-AD controls (Figure 5B), supporting the hypothesis that the presence of autoantibodies targeting MTBD-tau is unrelated to AD or other neurological disorders.

Systemic disorders and anti-tau autoimmunity

We next assessed possible associations between tau autoimmunity and extraneural diseases, which we binned into 27 main groups of disorders (Figure 6A). After adjustment for multiple comparisons, $\alpha\tau$ immunoreactivity showed significant associations with vascular disorders (aRR 1.51, 95% CI 1.28-1.77, P<0.001), nutritional disorders (aRR 1.31, 95% CI 1.14-1.50, P<0.001), anemia (aRR 1.49, 95% CI 1.21-1.82, P<0.001), kidney disorders (aRR 1.27, 95% CI 1.10-1.45, P=0.001) and urinary disorders (aRR 1.40, 95%CI 1.20-1.63, P<0.001) (Figure 6A), whereas no association was observed among patients with autoimmune disorders (Supplemental Figure 3). There was no difference in the coincidence of all comorbidities between $\alpha\tau^+$ samples (5, 0.46%) and $\alpha\tau^-$ samples (69, 0.33%) (P=0.633).

To address potential biases arising from grouping and selecting major categories, we explored the association between $\alpha\tau^+$ and individual ICD-10 codes. Across 276 individual ICD-10 codes and after correction for multiple comparisons, eight exhibited significant associations with $\alpha\tau^+$ (Figures 6B and C). These included "E61–deficiency of other nutrient elements" (aRR 2.22, 95% CI 1.54-3.06, P<0.001), "I74–arterial embolism and thrombosis*"* (aRR 2.09, 95% CI 1.40-2.94, P<0.001), "N30–cystitis" (aRR 1.84, 95% CI 1.32-2.47, P<0.001), "I70–atherosclerosis*"* (aRR 1.57, 95% CI 1.29-1.89, P<0.001), "D50–iron deficiency anemia*"* (aRR 1.50, 95% CI 1.21-1.82, P<0.001), "N39–other urinary disorders" (aRR 1.40, 95% CI 1.19-1.64, P<0.001), "B96–other bacterial agents as the cause of diseases*"* (aRR 1.40, 95% CI 1.17-1.66, P<0.001) and "N18–chronic kidney disease*"* (aRR 1.38, 95% CI 1.18-1.60, P<0.001; Figure 6C). Conversely, we found no significant negative association between tau autoreactivity and any ICD-10 codes that could suggest a decreased risk for a specific disease in $\alpha\tau^+$ patients (Figure 6C). To verify relevant associations, we used Bayesian logistic regression using logit-transformed EC_{50} values (-logit[EC_{50}]) as a continuous outcome. All the previously referred eight ICD-10 codes showed positive associations with -logit[EC_{50}] (Figure 6D).

To validate these conditions as significant associations with plasma MTBD-tau IgG autoantibodies, we examined the association between $\alpha\tau^+$ and 106 commonly requested laboratory parameters (Supplemental Table 2) using data available for 24,177 patients, independently of any ICD-10 classifiers. After correction for multiple comparisons, the laboratory markers "Leukocytes, urine", "Potassium" and "Urea" were positively associated with tau autoimmunity (Figure 6E). The association with increasing levels of urea and potassium suggests a link to kidney failure, whereas leukocytes in urine are a feature of urinary tract infections. These findings support the hypothesis that anti-tau autoimmunity correlates with such disorders. Accordingly, the prevalence of chronic

kidney disease was 12.4% in $\alpha\tau^-$ and 17.7% in $\alpha\tau^+$ patients, whereas that of other urinary disorders was 10.3% in $\alpha\tau^-$ and 15.1% in $\alpha\tau^+$ patients (Figure 6F).

DISCUSSION

This study was designed to discover novel associations between autoreactivity to tau and human diseases. This approach of "reverse immunopathology" is hypothesis-free: it does not pose constraints on the type of diseases that might result from anti-tau immunity. While the approach is generally applicable to any autoantigen, its predictive power relies on the analysis of large patient collectives, which in turn requires the development of high-throughput methods at reasonable cost. We therefore miniaturized antibody detection to 3 µl/sample in 1,536-well microplates, allowing to run 40,000 assays/24 hrs with minimal hands-on time. We performed >300,000 immunoassays on >40,000 plasma samples for ατ autoreactivity. Each sample was measured at eight dilution points, enabling precise and unambiguous titer determinations (24-26).

Plasma ατ IgG were more prevalent in women and increased with age, reaching 7.6% in the cohort of 90-99-year-olds. The specificity of $\alpha\tau^+$ plasma to MTBD-tau was high and was confirmed by multiple assays including epitope mapping. The age- and sex-adjusted $\alpha\tau^+$ rate in hospital patients was three-fold higher than in healthy blood donors and was 2.4 times higher than that of autoantibodies targeting other intracellular neuronal targets, suggesting a correlation with disease states (33). However, we did not find any association between $\alpha\tau^+$ and any neurological conditions including neurodegenerative diseases, corroborating with reports of similar levels of plasma tau autoantibodies in AD patients and non-demented controls (34). Instead, we uncovered a robust, specific association between $\alpha\tau^+$ positivity and kidney and urinary disorders. This was independently

validated by associations with higher prevalence of positive samples from the department of Nephrology, grouped kidney and urinary diseases, individual kidney and urinary diagnosis codes and related clinical laboratory biomarkers, such as high serum urea and potassium and high urine leukocytes.

Seroepidemiological studies cannot establish causality: ατ seropositivity could be a cause or a consequence of the clinical syndromes associated with it (35). However, tau is expressed in extraneural tissues, including kidney podocytes and urinary bladder (2-5), and its ablation causes glomerular pathologies (36). Besides raising the possibility that plasma ατ autoantibodies might drive kidney pathologies, these findings suggest that such autoantibodies represent useful biomarkers of these diseases and that it will be important to monitor renal and urinary function in the current clinical trials of tau immunotherapy (37-39).

Recent studies have explored the use of tau measurements in plasma as biomarkers for AD diagnosis and for monitoring its progression (9-12, 31, 40-44) However, we found that anti-MTBD-tau autoantibodies could hinder tau detection in plasma by binding to epitopes recognized by commercial biomarker immunoassays. This aligns with prior research indicating that both plasma anti-tau autoantibodies and administered anti-tau antibodies can influence the dynamics of tau levels in plasma (45). Additionally, a recent community cohort study using an immunoassay for AD screening revealed associations between plasma tau levels and numerous comorbidities, with chronic kidney disease showing one of the strongest associations (46). These results imply that the presence of anti-tau autoantibodies in plasma might impact the effectiveness of plasma tau as an AD biomarker. This consideration may become crucial as plasma tau levels move toward routine clinical use in AD diagnosis.

Limitations

Our large-scale assessment of plasma tau autoimmunity has certain limitations. Firstly, most samples analyzed in our study came from a university hospital cohort, implying a bias towards complex pathologies and polymorbidities. To account for this, we included a vast collection of samples from healthy blood donors. Secondly, our study is confined to two sites within a single region with approximately 1,500,000 inhabitants whose ethnic composition was not thoroughly examined. Additionally, a direct comparison of the prevalence of plasma anti-tau antibodies in these two cohorts may potentially suffer from variations in materials, collection methods (e.g. addition of heparin that may cause aggregation of MTBD-tau), and handling processes at the two different sites. Thirdly, our study is restricted to the analysis of specific disease groups, the absence of a replication cohort and a longitudinal disease cohort that would allow for verification, examining a time course, origin, and causal role of these autoantibodies. Fourthly, the statistical analysis of the association of MTBD-tau-autoreactivity and different disorders was based on ICD-10, a medical classification focused on reimbursement and cause-of-death statistics (47). We therefore performed additional statistical analyses using laboratory parameters, which have provided further support for the association of tau autoimmunity and systemic disorders.

Finally, we used bacterially expressed MTBD-tau as target, thereby excluding full-length or post-translationally modified tau epitopes, like the phosphorylated forms p-tau181 (48) and p-tau217 (49), that are increasingly used as biomarkers for AD diagnosis. As a result, our methodology may miss plasma anti-tau autoantibodies associated with AD pathology and could underestimate the prevalence of total anti-tau autoantibodies. Furthermore, this approach may introduce a bias towards detecting autoantibodies targeting total peripheral tau which is more abundant in plasma (50). Therefore, further studies with larger AD patient cohorts may be needed to more robustly

assess the prevalence of autoantibodies selectively targeting brain-derived tau and to support our hypotheses.

Conclusions

Our study identified a high seroprevalence of anti-MTBD-tau IgG autoantibodies in both plasma samples from university hospital patients and healthy blood donors. Tau autoimmunity is associated with female sex, older age and previously unrecognized extraneural diseases. These findings point to unrecognized roles for tau and anti-tau autoantibodies in extraneural pathologies.

MATERIALS AND METHODS

METHODS

Sex as a biological variable

Plasma samples from patients of both sexes were examined in this study.

Study design

From December 2017 until February 2020, residual heparin plasma samples were obtained from the Department of Clinical Chemistry, University Hospital of Zurich, USZ, Switzerland. Samples were collected during routine clinical care from patients admitted either as inpatients or outpatients (age ≥ 18 years) and were only included if basic demographic data was available, and an informed consent for research had been provided. From March until July 2020, EDTA plasma samples from blood donors were obtained from the Blood Donation Center of Zurich, Switzerland, according to standard criteria of blood donation. Exclusion criteria were as reported (24). Plasma samples were biobanked locally and tested in an automated indirect microELISA (Enzyme-Linked Immuno-sorbent Assay) ((24-26) and below) for natural IgG autoantibodies against the microtubule-binding-domain of tau (MTBD-tau, tauK18). Demographic and clinical data for the hospital cohort was obtained from clinical records of the USZ with follow-up until December 2021, while detailed clinical data for the blood donor cohort were not available for this study. ICD-10 codes (51) were used for clinical data assessment. AD patients were selected using ICD-10 code F00 or G30. Non-neurodegeneration controls were defined by the lack of any Fxx or Gxx ICD-10 codes.

Automated microELISA screen

Plasma samples were tested for natural anti-MTBD-tau IgG autoantibodies in a microELISA screen (24-26). Briefly, high-binding 1,536-well microplates (Perkin Elmer, SpectraPlate 1536

HB) were coated with 1 µg/mL of recombinant MTBD-tau (37 °C, 60 min). Plates were washed 3x with phosphate-buffered saline 0.1% Tween®20 (PBST) using a Biotek El406 washer-dispenser and blocked with 5% milk (Migros)-PBST (90 min). Plasma samples were diluted 1:20 in 1% milk-PBST and dispensed into the MTBD-tau-coated plates using ultrasound dispensing with an ECHO 555 Liquid Handler (Labcyte/Beckman Coulter). Each sample was tested at eight serial two-fold dilutions (1:50 to 1:6,000) using different volumes to a final volume of 3 µL/well. Human IgG-depleted serum (MyBioSource) was used as negative and anti-tau RD4 (4-repeat isoform) mouse monoclonal antibody (29) (05-804 clone 1E1/A6 Merck Millipore) as positive control. Plates were incubated (120 min, room temperature (RT)) and washed 5x with PBST. Secondary antibody peroxidase AffiniPure® goat anti-mouse IgG H+L (115-035-003, Jackson ImmunoResearch) at 1:2,000 dilution in 1% milk-PBST for the RD4 positive control, peroxidase AffiniPure® goat anti-human IgG Fcγ-specific (109-035-098, Jackson ImmunoResearch) 1:4,000 dilution in 1% milk-PBST for the plasma samples and the IgG-depleted serum negative control were dispensed into the plates using a Biotek MultifloFX dispenser. Plates were incubated (60 min, RT) and washed 3x with PBST. 3,3',5,5'-Tetramethylbenzidine (TMB) Chromogen Solution for ELISA (Invitrogen) was added as colorimetric horseradish peroxidase (HRP) substrate (3 min, RT). Finally, 0.5 M H_2SO_4 was added to stop the reaction. Plates were briefly centrifuged after each dispensing step except after dispensing of TMB. Plates were read at Optical Density (OD) = 450 nm in a plate reader (Perkin Elmer, Envision).

For the replicability assessment, 308 samples were tested in duplicates, running the replicates on the same day but using different 1536-well assay (destination) plates, different plate coordinates for each replicate, and calculating the $-\log_{10}(EC_{50})$ of each replicate independently.

Non-specific cross-reactivity was assessed by testing plasma samples against MTBD-tau and amyloid-ß pyroglutamate (13,099 hospital patients' plasma samples) and the cellular prion protein (PrP^C) (12,297 hospital patients' samples) using a similar protocol as described above.

Production and purification of recombinant tau

The gene encoding the human truncated 4R-tau corresponding to the microtubule binding domain of tau protein (MTBD-tau) was cloned into a pRSET-A plasmid (Invitrogen). For protein expression the respective vector was transformed into *E.coli* BL21(DE3) cells. Bacterial cells were grown in Luria Broth (LB) medium (Invitrogen) at 37 °C until an OD_{600} of 0.8 was reached and were then induced with isopropyl-β-D-thiogalactoside (IPTG) at a final concentration of 1 mM. After growing the cells for additional 6 h at 37 °C, cultures were harvested by centrifugation (6,000*g*, 10 min, 4 °C). Pellets were suspended in 20 mM piperazine-N,N-bis(2-ethanesulfonic) acid (PIPES), pH 6.5, 1 mM ethylenediaminetetraacetic acid (EDTA) and 50 mM 2-mercaptoethanol buffer and sonicated for 30 min at 4 °C. NaCl to 500 mM final concentration was added, samples were boiled at 95 °C for 20 min and centrifuged (9,000*g*, 30min, 4 °C). Ammonium sulfate was slowly added to a final concentration of 55% m/v and stirred for 1 h at room temperature (RT). Samples were centrifuged (15,000*g*, 10min, 4 °C), pellets were resuspended in 20 mM 4-(2-hydroxyethyl)piperazine-1-ethanesulfonic acid (HEPES) (pH 7.0), 2 mM dithiothreitol (DTT), passed through a 0.45 µm Acrodisc® filter (Sigma) and loaded onto Sepharose SP Fast Flow resin (Cytiva). Tau was eluted using a linear salt gradient from 0 to 1 M NaCl in 20 mM HEPES, pH 7.0, 2 mM DTT. Fractions containing tau were concentrated using Amicon® Ultra-15 centrifugal filter unit (10-kDa MWCO) (Merck) and dialyzed overnight at 4°C against phosphate-buffered saline (PBS, pH 7.4) (Kantonsapotheke Zurich), 1mM DTT. Pooled samples were passed through a HiLoad 26/60

Superdex75 (GE Healthcare) column. Protein samples were analyzed by SDS-PAGE and samples containing tau were concentrated using an Amicon® Ultra-15 centrifugal filter unit (10-kDa MWCO). Samples were assessed by SDS-PAGE and electrospray ionization-mass spectrometry (Functional Genomics Center Zurich, Switzerland). Pure MTBD-tau samples were stored until further use at -80°C. The concentration of tau was determined using a bicinchoninic acid assay (Pierce BCA Protein Assay Kit, Thermo Fisher).

For the purification of full-length tau, a similar protocol was used with the following changes. The gene encoding the longest 4R isoform of human full-length tau protein, tau^{441}, (tau/pET29b, Addgene #16316, gift from Peter Klein (52)) was cloned into a pRSET-A plasmid (Invitrogen). For protein expression, E.*coli* BL21(DE3)pLysS cells were transformed with the pRSET-A plasmid encoding tau^{441}. Cells were grown in Overnight Express™ Instant TB media (Novagen) for 6 h at 37 °C and then 12 h at 25 °C. Fractions containing full-length tau were concentrated using Amicon® Ultra-15 centrifugal filter unit (30-kDa MWCO) (Merck).

Purification of anti-tau autoantibodies from patient samples

Heparin plasma (between 3 mL and 20 mL per hospital cohort patient) was diluted 1:3.3 in PBS, and centrifuged (6,000 *g*, 10 min, 4 °C). The supernatant was loaded on a column containing 3 mL of epoxy-MTBD-tau (prepared with a previous overnight incubation of MTBD-tau and epoxy resin in a binding buffer of 0.1 M NaH_2PO_4–NaOH, 1 M NaCl, pH 9.2) by repetitive loading of the plasma sample overnight at 4 °C. The column was washed with 50 mL of PBS, and MTBD-tau autoantibodies were eluted four times with 5 mL 0.1 M glycine–HCl, pH 2.5, and immediately neutralized to pH 7.0 with 1 M Tris-HCl. Fractions containing antibodies against MTBD-tau were identified using an indirect colorimetric ELISA. Fractions containing the eluted antibodies were

stepwise concentrated using Amicon® Ultra-15, Ultra-4, and Ultra-0.5 mL centrifugal filter units (50-kDa MWCO) to up to a volume of 1 mL.

Competitive ELISA

High-binding 384-well plates (Perkin Elmer, SpectraPlate 384 HB) were coated with 4 µg/mL BT2 tau monoclonal antibody (#MN1010, Thermo Fisher) in PBS. Recombinant human tau^{441} (rPeptide) was diluted to a final concentration of 0.015 ng/mL and incubated with purified anti-tau autoantibodies four-fold serially diluted (1:1.66 to 1:106.6) in 1:2 plasma under rotation (500 rpm, 120 min, 37°C). Samples were transferred to BT2-coated plates and incubated (45 min, RT). After washing 4x with PBST, plates were incubated (0.125 µg/mL, 45 min, RT) with ab64193 (polyclonal IgG antibody; Abcam). Plates were washed 4x with PBST and incubated (1:2,000 dilution, 60 min, RT) with peroxidase AffiniPure® goat anti-Rabbit IgG (H+L) (111-035-045, Jackson ImmunoResearch). Plates were washed 4x with PBST and 1-Step™ Ultra TMB-ELISA solution (Thermo Fisher) was added (7 min, RT). After addition of 0.5 M H_2SO_4, plates were read at OD = 450 nm in a plate reader (Perkin Elmer, Envision).

For the competitive ELISAs of MTBD-tau autoantibodies, high-binding 384-well plates (Perkin Elmer, SpectraPlate 384 HB) were coated with 20 µL of 0.5 µg/mL of MTBD-tau at 4 °C overnight. Afterwards, plates were washed 3x with PBST with a Biotek El406 washer dispenser and blocked with 5% SureBlock™ (Lubio) in PBST for 120 min. Purified autoantibodies from hospital cohort patients' plasma were diluted 1:50 in 1% SureBlock™ (Lubio) in PBST (sample buffer). Anti-tau RD4 mouse monoclonal antibody (05-804 clone 1E1/A6 Merck Millipore) was diluted to a final concentration of 0.4 µg/mL. Bovine serum albumin (Thermo Scientific), in house purified recombinant MTBD-tau, a pool of eight synthetic peptides covering the sequence of MTBD-tau

with 25 amino acids length and 10 amino acids of overlap (Genscript) (Figure 2 I) and an unrelated 25 amino acid length synthetic TREM2 (Triggering receptor expressed on myeloid cells 2) peptide (GenScript) were used as competing antigens. Antibody samples were incubated overnight at 4°C with serial 2-fold dilutions of antigens solutions in sample buffer from 20,000 nM to 2.44 nM final concentration. Antibody-antigen solutions were added to the plates and incubated for 45 min at RT. Plates were washed 3x with PBST using a Biotek El406 washer dispenser and secondary antibodies were added as follows: peroxidase AffiniPure® goat anti-Human IgG (H+L) (109-035-088, Jackson ImmunoResearch) diluted 1:3,000 and peroxidase AffiniPure® goat anti-mouse IgG H+L (115-035-003, Jackson ImmunoResearch) diluted 1:2,000. Secondary antibodies were incubated for 60 min at RT and then plates were washed plates 4x with PBST. TMB Chromogen Solution for ELISA (Invitrogen) was added to the plates and incubated for 7 min at RT. Finally, 0.5 M H_2SO_4 was added. Plates were briefly centrifuged after each dispensing step except after dispensing colorimetric substrate. Plates were read at OD = 450 nm in a plate reader (SpectraMax® Paradigm®, Molecular Devices).

Indirect ELISAs

To test for polyreactivity, purified anti-tau autoantibodies were tested by indirect ELISA against several antigens (53, 54). High-binding 384-well plates (Perkin Elmer, SpectraPlate 384 HB) were coated with 1 µg/mL of in house purified MTBD-tau in PBS, 10 µg/mL of double stranded DNA from calf-thymus (Sigma) in PBS, 10 µg/mL of lipopolysaccharides from E.*coli* O111:B4 (Sigma) in PBS, 5 µg/mL of human recombinant insulin (Sigma) in PBS, 10 µg/mL of bovine serum albumin (Thermo Fisher) in PBS, 2 µg/mL of cardiolipin solution from bovine heart (Sigma) in ethanol or left high-binding plates uncoated at 4 °C overnight. Plates were washed 3x with PBST using a

Biotek El406 washer dispenser and then blocked 5% SureBlock™ (Lubio) in PBST for 120 min at RT. The following samples serially diluted 1:1 in sample buffer were incubated for 120 min at RT: patient purified anti-tau autoantibodies were diluted 1:33, human IgG-depleted plasma (Bio-Source) was 1:50 diluted and used as a negative control, anti-DNP (Sigma) was diluted to a final concentration of 6 µg/mL and used as a positive control for cardiolipin, DNA and albumin coated plates, anti-tau RD4 mouse monoclonal antibody (05-804 clone 1E1/A6 Merck Millipore) was diluted to a final concentration of 6 µg/mL and used as a positive control for MTBD-tau coated plates, pooled plasma from 20 patients (Institute Clinical Chemistry (IKC), University Hospital Zurich) was diluted 1:25 and used as a positive control for insulin, lipopolysaccharides and un-coated plates. Plates were then washed 4x with PBS-T using a Biotek El406 washer dispenser. Secondary antibodies were diluted and incubated for 60 min at RT as follows: peroxidase Affini-Pure® goat anti-human IgG (H+L) (109-035-088, Jackson ImmunoResearch) diluted 1:3,000 and added to purified MTBD-tau autoantibodies and IKC pool wells, peroxidase AffiniPure® goat anti-mouse IgG H+L (115-035-003, Jackson ImmunoResearch) diluted 1:2,500 and added to anti-RD4 wells, and peroxidase AffiniPure® goat anti-rabbit IgG (H+L) (111-035-045, Jackson Im-munoResearch) diluted 1:4,000 and added to anti-DNP wells. Plates were washed plates 4x with PBST. TMB Chromogen solution for ELISA (Invitrogen) was incubated for 7 min at RT. Finally, 0.5 M H_2SO_4 was added. Plates were briefly centrifuged after each dispensing step except after dispensing colorimetric substrate. Plates were read at OD = 450nm in a plate reader (SpectraMax® Paradigm®, Molecular Devices).

For relative affinity measurements, we used a similar approach with the following modifications. An indirect ELISA in 384-well plates (Perkin Elmer, SpectraPlate 384 HB) with MTBD-tau as a coating antigen, was used. The starting concentration of all antibodies, assayed in triplicates, was

10 µg/mL. They were successively diluted 1:3 to reach a concentration of $2x10^{-6}$ µg/mL. As reference antibody, we used purified RD4 kindly provided by Prof. Rohan de Silva (UCL Queen Square Institute of Neurology, London, UK). As additional controls, we used anti-LAG3 (Lymphocyte Activation Gene 3) antibody Relatlimab (ant-LAG3) (24), $\alpha\tau^-$ plasma sample and uncoated plates. The respective EC_{50} values were determined using logistic regression, as described below.

For IgG subclassing, the following secondary antibodies were used: rabbit anti-human IgG1 (SA5-10202, Invitrogen), rabbit anti-human IgG2 (SA5-10203, Invitrogen), rabbit anti-human IgG3 (SA5-10204, Invitrogen) or rabbit anti-human IgG4 (SA5-10205, Invitrogen) diluted 1:1,500, peroxidase AffiniPure® goat anti-rabbit IgG (H+L) antibody (111-035-045, Jackson ImmunoResearch) diluted 1:2,500.

For immunoglobulin light chain typing, the following secondary antibodies were used: peroxidase goat anti-human κ 1:4,000 diluted (26), peroxidase goat anti-human λ 1:4,000 diluted (26).

For epitope mapping, a similar approach was used: high-binding 384-well plates (Perkin Elmer, SpectraPlate 384 HB) with 1 µg/mL of each individual MTBD-tau synthetic peptide (GenScript) diluted in PBS at 4 °C overnight. 8 synthetic peptides spanning the sequence of MTBD-tau with 25 amino acids length and 10 amino acids of overlap were used. Plasma samples were diluted 1:50, human IgG-depleted serum (MyBioSource) was 1:50 diluted and used as a negative control and anti-tau RD4 mouse monoclonal antibody (05-804 clone 1E1/A6 Merck Millipore) was diluted to a final concentration of 6 µg/mL and used as a positive control. The following secondary antibodies diluted in sample buffer were used: peroxidase AffiniPure® goat anti-human IgG (H+L) (109-035-088, Jackson ImmunoResearch) diluted 1:5,000 and peroxidase AffiniPure® goat anti-mouse IgG H+L (115-035-003, Jackson ImmunoResearch) diluted 1:2,500 and added to anti-RD4 wells.

For IgG subclassing, immunoglobulin light chain typing and epitope mapping experiments, we classified samples to be reactive if the OD_{450} was higher than the average of all negatives OD450 + 2x the standard deviation of the OD_{450} of the negatives.

Western blotting

SH-SY5Y wild-type cells (Sigma) and SH-SY5Y cells overexpressing double-mutant $tau^{P301L/S320F}$ were lysed in 0.5% Triton™ X-100 (Sigma Aldrich) in PBS, supplemented with cOmplete™ Mini EDTA-free Protease Inhibitor Cocktail (Roche) on ice and supernatant was recovered after centrifugation (14,000g, 20min, 4°C). Protein concentration was estimated using a bicinchoninic acid assay (Pierce BCA Protein Assay Kit, Thermo Fisher) and sample volumes were adapted to 30 µg of total protein. Samples were loaded onto NuPAGE 12% Bis-Tris gels (Invitrogen). Gels were loaded in the following repeating pattern: protein ladder, SH-SY5Y wt and SH-SY5Y $tau^{P301L/S320F}$ cell lysates. SDS-PAGE gels were run at 180 V in MES buffer for 45 min, transferred to nitrocellulose membranes (Invitrogen) using a dry transfer system (iBlot 2 Gel Transfer Device, Invitrogen, Thermo Fisher), membranes were cut vertically along the protein ladder and blocked with 5% SureBlock (Lubio Science) in PBST for 30 min at RT. Membranes were incubated with patient purified anti-tau autoantibodies 1:100 diluted in in 1% SureBlock in PBST overnight at 4 °C. Negative control membranes were not incubated with primary antibodies. Membranes were washed 3x for 5 min with PBST and then incubated with the following secondary antibodies for 60 min at RT: peroxidase AffiniPure® goat anti-mouse IgG H+L (115-035-003, Jackson ImmunoResearch) 1:10,000 and peroxidase AffiniPure® goat anti-human IgG (H+L) (109-035-088, Jackson ImmunoResearch) 1:10,000 diluted with 1% SureBlock in PBST. The negative control was only incubated with peroxidase goat anti-human secondary antibody. Monoclonal mouse anti-actin clone C4 (MAB1501R, Chemicon) diluted 1:10,000 in 1% SureBlock in PBST was used as a loading

control. Membranes were washed 4x for 5 min with PBST and developed using the Immobilon Crescendo HRP Substrate (Millipore). Individual membranes were imaged using the Fusion SOLO S imaging system (Vilber).

In vitro MTBD-tau aggregation assay

MTBD-tau *in vitro* aggregation experiments were performed as previously described (30). Briefly, 7 µM of in-house purified recombinant MTBD-tau, 3.5 µM of heparin (Santa Cruz Biotechnology) and 10 µM of thioflavin T (ThT, Sigma) were diluted in PBS. The patient purified anti-tau auto-antibodies and controls (plasma sample reactive against the LAG3 and IgG-purified using Protein G Sepharose (Cytiva)) were added at the indicated apparent stoichiometries in Figure 3. The mixtures with a total volume of 200 µl were added to black 96-well polystyrene microplates (Nunc, Prod. No. 265301) and ThT fluorescence (450/480 nm ex/em filters; bottom read mode) was measured at 37°C under continuous orbital shaking (425 cpm) every 15 min for 96 h using a FLUOstar Omega microplate reader (BMG Labtech). The mean baseline fluorescence values were subtracted from the mean fluorescence values at each time point which were then normalized to maximum baseline-subtracted fluorescence values and multiplied by 100 (55).

Statistical analysis

Antibody titers were defined as the negative logarithm half-maximal responses ($-\log_{10}(EC_{50})$) obtained by fitting the OD = 450 nm of the eight dilution points of each sample tested in the micro-ELISA to a logistic regression fitter. We classified as positives samples with a cut-off of $-\log_{10}(EC_{50}) \geq 1.8$ (24), corresponding to a nominal dilution of > 1/64. Non-informative samples (fitting error >20% $-\log_{10}(EC_{50})$ or high background) were excluded from the analysis (24). In

cases where more than one sample was available for the same individual the most recent $\log_{10}(EC_{50})$ value was used.

Age is presented as median with interquartile range (IQR) and comparisons were performed using non-parametric Mann-Whitney U test. Categorized age groups and sex of positives and negatives are shown as percentages and compared using two-proportions Z-test or χ^2 test for trend in proportions. Log-binomial regression models (27, 56) using MTBD-tau autoreactivity were employed to estimate age-and-sex adjusted RRs (aRR) and 95% confidence intervals (CIs), and to investigate the association between the detection of anti-MTBD-tau IgG autoantibodies and different demographic features.

For the AD cohort microELISA screen, $\log_{10}(EC_{50})$ values were compared using Mann-Whitney U test. Additionally, Bayesian logistic regression was conducted (24, 57-59), using $-\text{logit}_{10}(EC_{50})$ values as outcome, i.e. without dichotomising the outcome using the R package rstanarm and the following priors (prior=normal[0, 2.5, autoscale=TRUE],prior_intercept = normal[5000, 2.5, autoscale=TRUE)] prior_aux = exponential [1, autoscale =TRUE]. We aimed to confirm the positive association between ICD-10 codes previously identified using a conventional logistic regression model with high $-\log_{10}(EC_{50})$ values. Each ICD-10 code was analyzed in an independent logistic regression and adjusted for age and sex.

The association between MTBD-tau-autoreactivity and neurological and systemic disorders, respectively, was analysed by applying multivariate log-binomial regression models to estimate aRRs and 95% CIs. For neurological disorders, 23 major groups of ICD-10 codes (Supplemental Table 3) corresponding to neurological disorders identified at least once in the positive samples were used. For systemic disorders, the 27 major groups of ICD-10 codes (Supplemental Table 4) or 276 individual ICD-10 codes corresponding to systemic disorders identified at least once in the

positive samples and with at least 200 total counts were used to avoid overinterpretation of rare cases of disease. Individual disease entities with a P value < 0.05 Bonferroni corrected for multiple comparisons were included in a multivariate log-binomial regression analysis.

For the association between MTBD-tau-autoreactivity and clinical laboratory parameters, we used laboratory parameters with more than 2,000 total counts and calculated median values of the total values available for each patient in case of repetition of the clinical laboratory test. We used multivariate log-binomial regression models to estimate aRR and 95% CI using 106 clinical laboratory tests.

Statistical significance was defined by 2-tailed P-value ≤ 0.05. Statistical analyses and data visualization were performed using R version 4.3.2 and RStudio version 1.4.1106 (60).

Study approval

Collection of samples and clinical data were conducted according to study protocols approved by the Cantonal Ethics Committee of the Canton of Zurich, Switzerland (KEK-ZH Nr. 2015-0561, BASEC-Nr. 2018-01042, and BASEC-Nr. 2020-01731).

Data availability:

Data and material requests should be addressed to the corresponding authors. Materials will be shared upon approval by an ethics committee or review board and a material transfer agreement.

List of Supplementary Materials:

Supplemental Figure 1, 2, and 3

Supplemental Table 1, 2, 3 and 4

563

References

1. Gu Y, Oyama F, and Ihara Y. Tau is widely expressed in rat tissues. *J Neurochem.* 1996;67(3):1235-44.
2. Uhlen M, Fagerberg L, Hallstrom BM, Lindskog C, Oksvold P, Mardinoglu A, et al. Proteomics. Tissue-based map of the human proteome. *Science.* 2015;347(6220):1260419.
3. Sotiropoulos I, Galas MC, Silva JM, Skoulakis E, Wegmann S, Maina MB, et al. Atypical, non-standard functions of the microtubule associated Tau protein. *Acta Neuropathol Commun.* 2017;5(1):91.
4. Rinschen MM, Gödel M, Grahammer F, Zschiedrich S, Helmstädter M, Kretz O, et al. A Multi-layered Quantitative In Vivo Expression Atlas of the Podocyte Unravels Kidney Disease Candidate Genes. *Cell Rep.* 2018;23(8):2495-508.
5. Ho KH, Yang X, Osipovich AB, Cabrera O, Hayashi ML, Magnuson MA, et al. Glucose Regulates Microtubule Disassembly and the Dose of Insulin Secretion via Tau Phosphorylation. *Diabetes.* 2020;69(9):1936-47.
6. Kosik KS, Joachim CL, and Selkoe DJ. Microtubule-associated protein tau (tau) is a major antigenic component of paired helical filaments in Alzheimer disease. *Proc Natl Acad Sci U S A.* 1986;83(11):4044-8.
7. Joachim CL, Morris JH, Kosik KS, and Selkoe DJ. Tau antisera recognize neurofibrillary tangles in a range of neurodegenerative disorders. *Ann Neurol.* 1987;22(4):514-20.
8. Hanseeuw BJ, Betensky RA, Jacobs HIL, Schultz AP, Sepulcre J, Becker JA, et al. Association of Amyloid and Tau With Cognition in Preclinical Alzheimer Disease: A Longitudinal Study. *JAMA Neurol.* 2019;76(8):915-24.
9. Mattsson N, Zetterberg H, Janelidze S, Insel PS, Andreasson U, Stomrud E, et al. Plasma tau in Alzheimer disease. *Neurology.* 2016;87(17):1827-35.
10. Janelidze S, Mattsson N, Palmqvist S, Smith R, Beach TG, Serrano GE, et al. Plasma P-tau181 in Alzheimer's disease: relationship to other biomarkers, differential diagnosis, neuropathology and longitudinal progression to Alzheimer's dementia. *Nat Med.* 2020;26(3):379-86.
11. Mielke MM, Hagen CE, Wennberg AMV, Airey DC, Savica R, Knopman DS, et al. Association of Plasma Total Tau Level With Cognitive Decline and Risk of Mild Cognitive Impairment or Dementia in the Mayo Clinic Study on Aging. *JAMA Neurol.* 2017;74(9):1073-80.
12. Palmqvist S, Tideman P, Mattsson-Carlgren N, Schindler SE, Smith R, Ossenkoppele R, et al. Blood Biomarkers to Detect Alzheimer Disease in Primary Care and Secondary Care. *JAMA.* 2024.
13. Asuni AA, Boutajangout A, Quartermain D, and Sigurdsson EM. Immunotherapy targeting pathological tau conformers in a tangle mouse model reduces brain pathology with associated functional improvements. *J Neurosci.* 2007;27(34):9115-29.
14. Boutajangout A, Ingadottir J, Davies P, and Sigurdsson EM. Passive immunization targeting pathological phospho-tau protein in a mouse model reduces functional decline and clears tau aggregates from the brain. *J Neurochem.* 2011;118(4):658-67.
15. Congdon EE, and Sigurdsson EM. Tau-targeting therapies for Alzheimer disease. *Nat Rev Neurol.* 2018;14(7):399-415.

16. Rothstein TL. Natural Antibodies as Rheostats for Susceptibility to Chronic Diseases in the Aged. *Front Immunol.* 2016;7:127.
17. Lutz HU, Binder CJ, and Kaveri S. Naturally occurring auto-antibodies in homeostasis and disease. *Trends Immunol.* 2009;30(1):43-51.
18. Jaycox JR, Dai Y, and Ring AM. Decoding the autoantibody reactome. *Science.* 2024;383(6684):705-7.
19. Florance NR, Davis RL, Lam C, Szperka C, Zhou L, Ahmad S, et al. Anti-N-methyl-D-aspartate receptor (NMDAR) encephalitis in children and adolescents. *Ann Neurol.* 2009;66(1):11-8.
20. Lennon VA, Wingerchuk DM, Kryzer TJ, Pittock SJ, Lucchinetti CF, Fujihara K, et al. A serum autoantibody marker of neuromyelitis optica: distinction from multiple sclerosis. *Lancet.* 2004;364(9451):2106-12.
21. Ferrero J, Williams L, Stella H, Leitermann K, Mikulskis A, O'Gorman J, and Sevigny J. First-in-human, double-blind, placebo-controlled, single-dose escalation study of aducanumab (BIIB037) in mild-to-moderate Alzheimer's disease. *Alzheimers Dement (N Y).* 2016;2(3):169-76.
22. Bartos A, Fialová L, and Švarcová J. Lower Serum Antibodies Against Tau Protein and Heavy Neurofilament in Alzheimer's Disease. *J Alzheimers Dis.* 2018;64(3):751-60.
23. Kronimus Y, Albus A, Balzer-Geldsetzer M, Straub S, Semler E, Otto M, et al. Naturally Occurring Autoantibodies against Tau Protein Are Reduced in Parkinson's Disease Dementia. *PLoS One.* 2016;11(11):e0164953.
24. Emmenegger M, De Cecco E, Lamparter D, Jacquat RPB, Riou J, Menges D, et al. Continuous population-level monitoring of SARS-CoV-2 seroprevalence in a large European metropolitan region. *iScience.* 2023;26(2):105928.
25. Emmenegger M, Zografou C, Yile D, Hoyt LR, Gudneppanavar R, Chincisan A, et al. The Cystic Fibrosis Transmembrane Regulator Controls Tolerogenic Responses to Food Allergens in Mice and Humans. *medRxiv.* 2024.
26. Senatore A, Frontzek K, Emmenegger M, Chincisan A, Losa M, Reimann R, et al. Protective anti-prion antibodies in human immunoglobulin repertoires. *EMBO Mol Med.* 2020;12(9):e12739.
27. Diaz-Quijano FA. A simple method for estimating relative risk using logistic regression. *BMC Med Res Methodol.* 2012;12:14.
28. Donoghoe MW, and Marschner IC. Logbin: An R Package for Relative Risk Regression Using the Log-Binomial Model. *Journal of Statistical Software* 2018;86(21).
29. de Silva R, Lashley T, Gibb G, Hanger D, Hope A, Reid A, et al. Pathological inclusion bodies in tauopathies contain distinct complements of tau with three or four microtubule-binding repeat domains as demonstrated by new specific monoclonal antibodies. *Neuropathol Appl Neurobiol.* 2003;29(3):288-302.
30. Apetri A, Crespo R, Juraszek J, Pascual G, Janson R, Zhu X, et al. A common antigenic motif recognized by naturally occurring human V. *Acta Neuropathol Commun.* 2018;6(1):43.
31. Pase MP, Beiser AS, Himali JJ, Satizabal CL, Aparicio HJ, DeCarli C, et al. Assessment of Plasma Total Tau Level as a Predictive Biomarker for Dementia and Related Endophenotypes. *JAMA Neurol.* 2019;76(5):598-606.

32. Barini E, Plotzky G, Mordashova Y, Hoppe J, Rodriguez-Correa E, Julier S, et al. Tau in the brain interstitial fluid is fragmented and seeding-competent. *Neurobiol Aging.* 2022;109:64-77.
33. Dahm L, Ott C, Steiner J, Stepniak B, Teegen B, Saschenbrecker S, et al. Seroprevalence of autoantibodies against brain antigens in health and disease. *Ann Neurol.* 2014;76(1):82-94.
34. Yu G, Chen J, Xu Y, Zhu C, Yu H, Liu S, et al. Generation of goats lacking prion protein. *Mol Reprod Dev.* 2009;76(1):3.
35. Tsuboi Y, Uitti RJ, Delisle MB, Ferreira JJ, Brefel-Courbon C, Rascol O, et al. Clinical features and disease haplotypes of individuals with the N279K tau gene mutation: a comparison of the pallidopontonigral degeneration kindred and a French family. *Arch Neurol.* 2002;59(6):943-50.
36. Vallés-Saiz L, Peinado-Cahuchola R, Ávila J, and Hernández F. Microtubule-associated protein tau in murine kidney: role in podocyte architecture. *Cell Mol Life Sci.* 2022;79(2):97.
37. Congdon EE, Ji C, Tetlow AM, Jiang Y, and Sigurdsson EM. Tau-targeting therapies for Alzheimer disease: current status and future directions. *Nat Rev Neurol.* 2023;19(12):715-36.
38. ClinicalTrial.gov N, Dominantly Inherited Alzheimer Network Trial: An Opportunity to Prevent Dementia. A Study of Potential Disease Modifying Treatments in Individuals With a Type of Early Onset Alzheimer's Disease Caused by a Genetic Mutation (DIAN-TU). https://clinicaltrials.gov/study/NCT05269394?cond=Alzheimer%20Disease&term=E2814&rank=1; 2023.
39. Barton ME, Van Den Steen B, Van Tricht HLG, Byrnes W, Purcell FE, Southcott SA, et al. Update on the TOGETHER study: a patient- and investigator-blind, randomized, placebo-controlled study evaluating the efficacy, safety and tolerability of bepranemab, UCB0107, in prodromal-to-mild Alzheimer's disease. *Alzheimer's & Dementia.* 2022;18(S10):e068973.
40. Moscoso A, Grothe MJ, Ashton NJ, Karikari TK, Lantero Rodríguez J, Snellman A, et al. Longitudinal Associations of Blood Phosphorylated Tau181 and Neurofilament Light Chain With Neurodegeneration in Alzheimer Disease. *JAMA Neurol.* 2021;78(4):396-406.
41. Barthélemy NR, Li Y, Joseph-Mathurin N, Gordon BA, Hassenstab J, Benzinger TLS, et al. A soluble phosphorylated tau signature links tau, amyloid and the evolution of stages of dominantly inherited Alzheimer's disease. *Nat Med.* 2020;26(3):398-407.
42. Karikari TK, Pascoal TA, Ashton NJ, Janelidze S, Benedet AL, Rodriguez JL, et al. Blood phosphorylated tau 181 as a biomarker for Alzheimer's disease: a diagnostic performance and prediction modelling study using data from four prospective cohorts. *Lancet Neurol.* 2020;19(5):422-33.
43. Park JC, Han SH, Yi D, Byun MS, Lee JH, Jang S, et al. Plasma tau/amyloid-β1-42 ratio predicts brain tau deposition and neurodegeneration in Alzheimer's disease. *Brain.* 2019;142(3):771-86.
44. Palmqvist S, Janelidze S, Quiroz YT, Zetterberg H, Lopera F, Stomrud E, et al. Discriminative Accuracy of Plasma Phospho-tau217 for Alzheimer Disease vs Other Neurodegenerative Disorders. *JAMA.* 2020;324(8):772-81.

45. Yanamandra K, Patel TK, Jiang H, Schindler S, Ulrich JD, Boxer AL, et al. Anti-tau antibody administration increases plasma tau in transgenic mice and patients with tauopathy. *Sci Transl Med.* 2017;9(386).
46. Mielke MM, Dage JL, Frank RD, Algeciras-Schimnich A, Knopman DS, Lowe VJ, et al. Performance of plasma phosphorylated tau 181 and 217 in the community. *Nat Med.* 2022;28(7):1398-405.
47. St Germaine-Smith C, Metcalfe A, Pringsheim T, Roberts JI, Beck CA, Hemmelgarn BR, et al. Recommendations for optimal ICD codes to study neurologic conditions: a systematic review. *Neurology.* 2012;79(10):1049-55.
48. Meng J, and Lei P. Plasma pTau181 as a biomarker for Alzheimer's disease. *MedComm (2020).* 2020;1(1):74-6.
49. Telser J, Risch L, Saely CH, Grossmann K, and Werner P. P-tau217 in Alzheimer's disease. *Clin Chim Acta.* 2022;531:100-11.
50. Gonzalez-Ortiz F, Turton M, Kac PR, Smirnov D, Premi E, Ghidoni R, et al. Brain-derived tau: a novel blood-based biomarker for Alzheimer's disease-type neurodegeneration. *Brain.* 2023;146(3):1152-65.
51. Organization WH. 2004.
52. Hedgepeth CM, Conrad LJ, Zhang J, Huang HC, Lee VM, and Klein PS. Activation of the Wnt signaling pathway: a molecular mechanism for lithium action. *Dev Biol.* 1997;185(1):82-91.
53. Bunker JJ, Erickson SA, Flynn TM, Henry C, Koval JC, Meisel M, et al. Natural polyreactive IgA antibodies coat the intestinal microbiota. *Science.* 2017;358(6361).
54. Mouquet H, Scheid JF, Zoller MJ, Krogsgaard M, Ott RG, Shukair S, et al. Polyreactivity increases the apparent affinity of anti-HIV antibodies by heteroligation. *Nature.* 2010;467(7315):591-5.
55. Orru CD, Yuan J, Appleby BS, Li B, Li Y, Winner D, et al. Prion seeding activity and infectivity in skin samples from patients with sporadic Creutzfeldt-Jakob disease. *Sci Transl Med.* 2017;9(417).
56. McNutt LA, Wu C, Xue X, and Hafner JP. Estimating the relative risk in cohort studies and clinical trials of common outcomes. *Am J Epidemiol.* 2003;157(10):940-3.
57. Emmenegger M, Emmenegger V, Shambat SM, Scheier TC, Gomez-Mejia A, Chang CC, et al. Antiphospholipid antibodies are enriched post-acute COVID-19 but do not modulate the thrombotic risk. *Clin Immunol.* 2023;257:109845.
58. M. Emmenegger VE, in Zenodo, 2023. https://doi.org/10.5281/zenodo.10051979. .
59. Losa M, Emmenegger M, De Rossi P, Schurch PM, Serdiuk T, Pengo N, et al. The ASC inflammasome adapter governs SAA-derived protein aggregation in inflammatory amyloidosis. *EMBO Mol Med.* 2024;16(9):2024-42.
60. RStudioTeam. (RStudio P, Boston, MA, 2021).

Acknowledgments:

The authors wish to thank the hospital patients and blood donors for their generous altruistic contributions to this study. Imaging was performed with equipment maintained by the Center for Microscopy and Image Analysis, University of Zurich. We thank Prof. Rohan de Silva (UCL Queen Square Institute of Neurology, London, UK) for providing the purified anti-MTBD-tau antibody RD4. We thank Dr. Marco Losa for the generous provision of secondary antibodies for light chain typing and Magdalena Bialkowska, Lisa Caflisch, Berre Doğançay, Julie Domange, Marigona Imeri, Lorène Mottier, Rea Müller, Antonella Rosati, Dezirae Schneider, and Anne Wiedmer for help with the high-throughput assays. Insightful advice about programming in R software was provided by Reto Guadagnini.

Funding:

University of Zürich, Candoc grant FK-19-025 (ADM)

Swiss Personalised Health Network, SPHN, driver project grant 2017DRI17 (AA)

Swiss National Foundation SNF (SNSF grant ID 179040 and grant ID 207872, Sinergia grant ID 183563) (AA)

European Research Council ERC Prion2020, 670958 (AA)

Nomis Foundation (AA)

Innovation Fund of the University Hospital Zurich (INOV00096) (AA)

University Hospital Zurich Foundation grant USZF27101 (with contributions of the NOMIS Foundation, the Schwyzer Winiker Stiftung, and the Baugarten Stiftung, AA, ME)

HMZ ImmunoTarget grant, Stiftung Neuropath and GELU Foundation (AA)

Michael J. Fox Foundation (grant ID MJFF-020710 and MJFF-021073) (SH).

Author contributions:

Conceived and designed the experiments: ADM, SH, AA. Supervised the study: SH, AA. Performed tau protein purification: ADM, EDC, JG. Performed tau microELISA automated screen: ADM, ME. Performed amyloid-ß pyroglutamate and cellular prion protein microELISA automated screen: MC, KF, ME. Maintained microELISA automated platform: ME. Performed purification, validation and characterization of anti-tau autoantibodies: ADM, JG. Maintained the clinical database: ME, AC. Performed data analysis and visualization: ADM. Wrote the first draft of manuscript: ADM. Corrected and advised on subsequent versions of the manuscript: ADM, ME, SH, AA. All authors reviewed and approved the final version of the manuscript and consented to be accountable for the work.

Figures

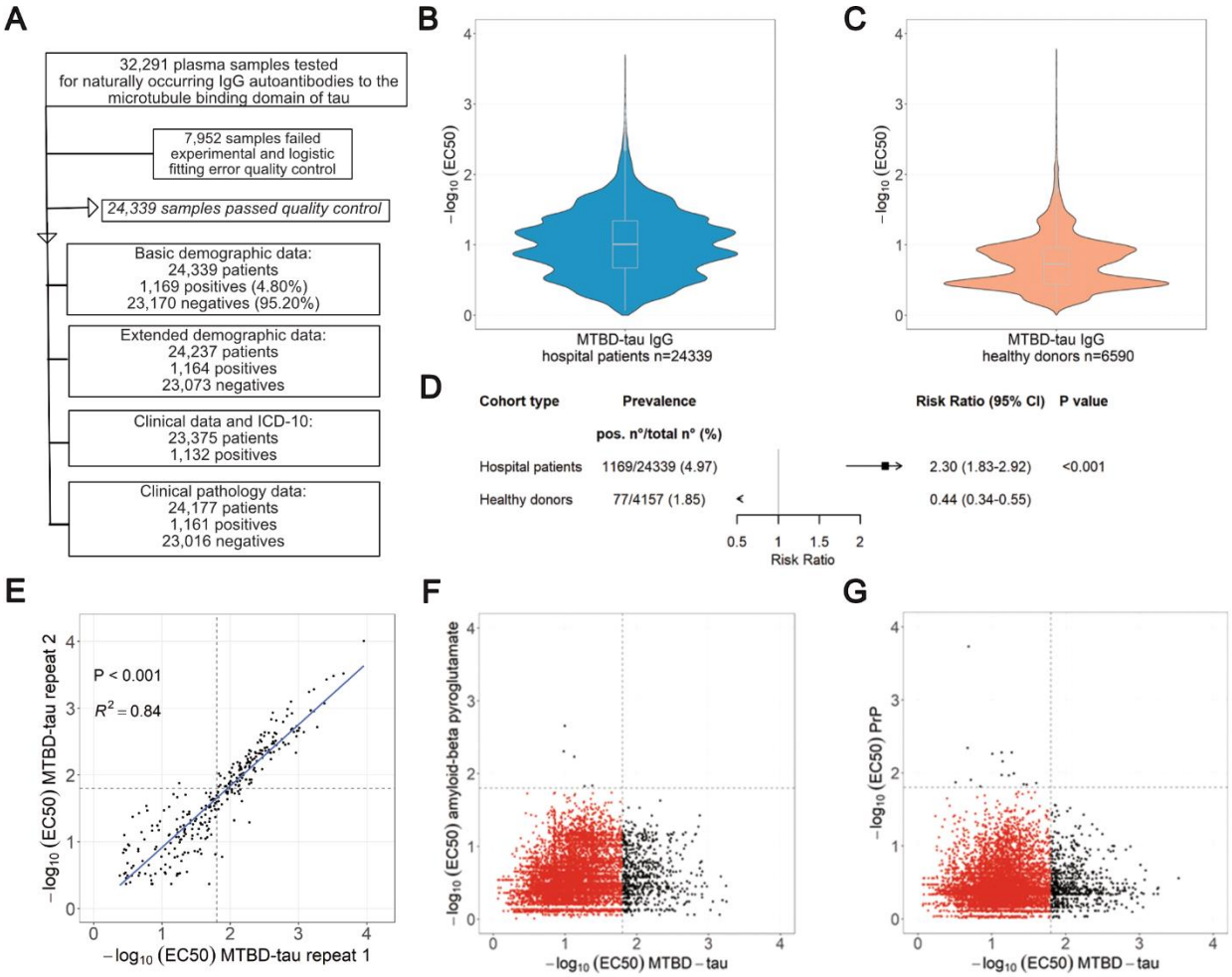

Figure 1. Study overview and seroprevalence of anti-MTBD-tau IgG autoantibodies. A. Flowchart of the study design. **B.-C.** Distribution of $-\log_{10}(EC_{50})$ values obtained from the micro-ELISA screen of hospital (B) and blood donor (C) plasma samples. **D.** Age- and sex-adjusted risk ratio ratios and 95% confidence intervals (CI; I bars) for the detection of anti-tau autoantibodies in hospital and blood-bank plasma samples. **E.** Replicability of microELISA duplicates with independent estimation of the $-\log_{10}(EC_{50})$ values. Dashed lines: cut-off value of $-\log_{10}(EC_{50}) = 1.8$. **F.** $-\log_{10}(EC_{50})$ values of samples tested by microELISA against MTBD-tau and amyloid-ß pyroglutamate. **G.** Same as shown in (F), but for samples tested against MTBD-tau and the cellular prion protein (PrP^{C}).

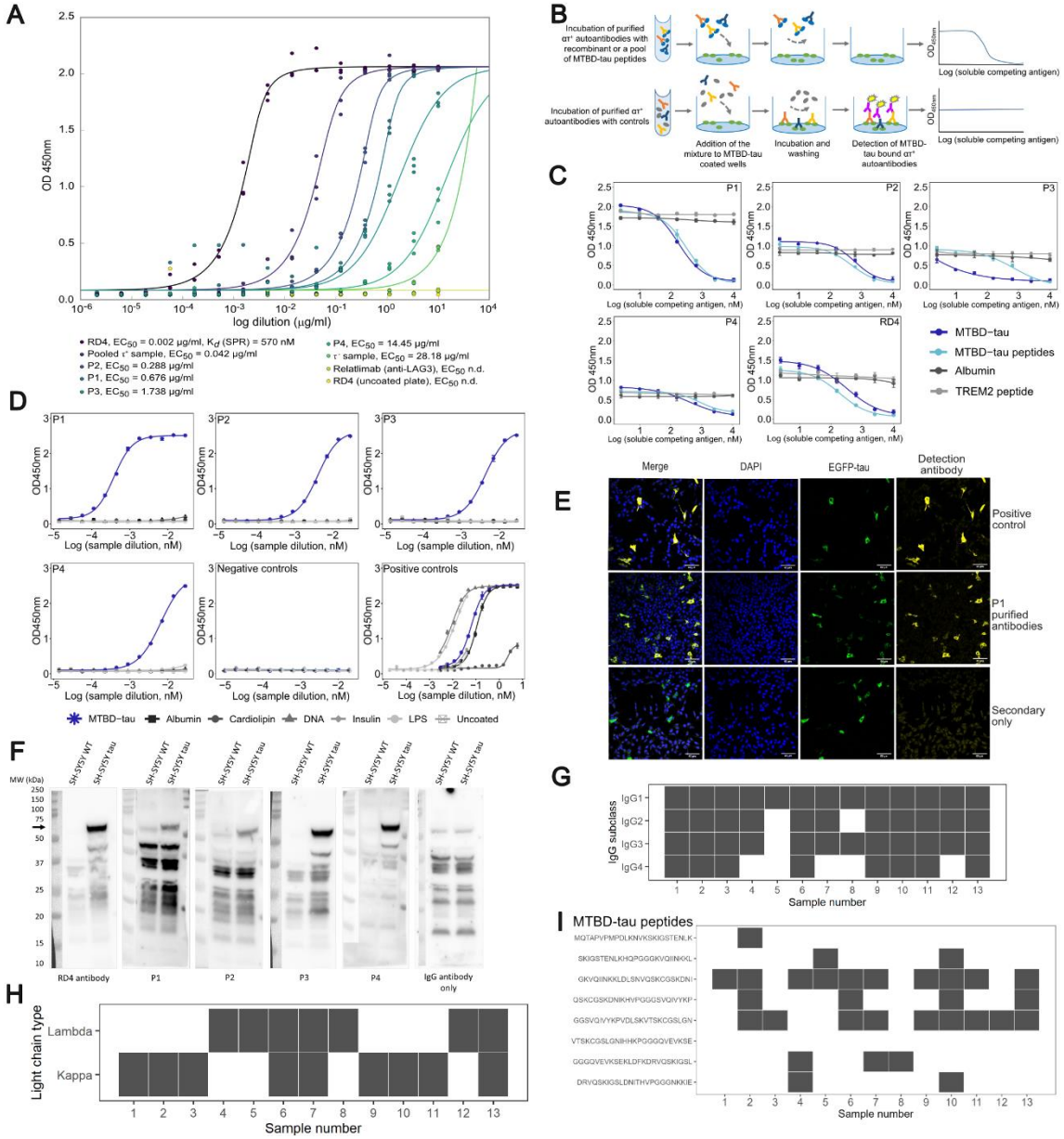

Figure 2. Biophysical characterization of samples from ατ⁺ patients. A. Indirect ELISA of purified anti-MTBD-tau autoantibodies from four $\alpha\tau^+$ samples and from 6 pooled $\alpha\tau^+$ samples. All antibodies were assayed at the same concentration to compare their EC_{50} to that of RD4. Relatimab (anti-LAG3) was used as negative control. EC_{50} values are indicated in the Figure. n.d.: not determined. **B.** Principle of competition ELISA. **C.** Competition ELISA of purified anti-tau autoantibodies from four $\alpha\tau^+$ patients against albumin, recombinant MTBD-tau, a pool of synthetic peptides spanning the sequence of MTBD-tau and synthetic TREM2. RD4 antibody: positive control. Mean values ± SD of two replicates. **D.** Indirect ELISA to assess the reactivity of purified anti-tau autoantibodies against albumin, cardiolipin, double-stranded DNA, insulin, lipopolysaccharides

(LPS), MTBD-tau and uncoated plates. Positive controls were as follows: RD4 antibody for MTBD-tau, anti-DNP antibody for cardiolipin, albumin and DNA and the IKC pool of 20 heparin plasma samples for insulin, LPS and uncoated plates. Mean values ± SD of two replicates are shown. **E.** Representative immunofluorescence images of SH-SY5Y cells expressing EGFP-0N4R-tau using affinity-purified anti-tau autoantibodies. HT7 pan-tau antibody: positive control. No primary antibody: negative control. Scale bar: 60 µm. **F.** Western blot of cell lysates from wild-type (SH-SY5Y WT) or tau$^{P301L/S320F}$-overexpressing cells (SH-SY5Y tau) using purified anti-tau autoantibodies from four $\alpha\tau^{+}$ patients. Positive control: RD4. Negative control: omission of primary antibody. **G.** IgG subclass typing of 13 $\alpha\tau^{+}$ plasma samples. Gray and white boxes: reactive and non-reactive samples, respectively. **H.** κ/λ light chain typing of the samples in F. **I.** Epitope mapping of the samples in Figure 2F against 25mer MTBD-tau peptides with 10 residues overlap. Vertical axis: sequences of the MTBD-tau peptides covering the sequence of MTBD-tau.

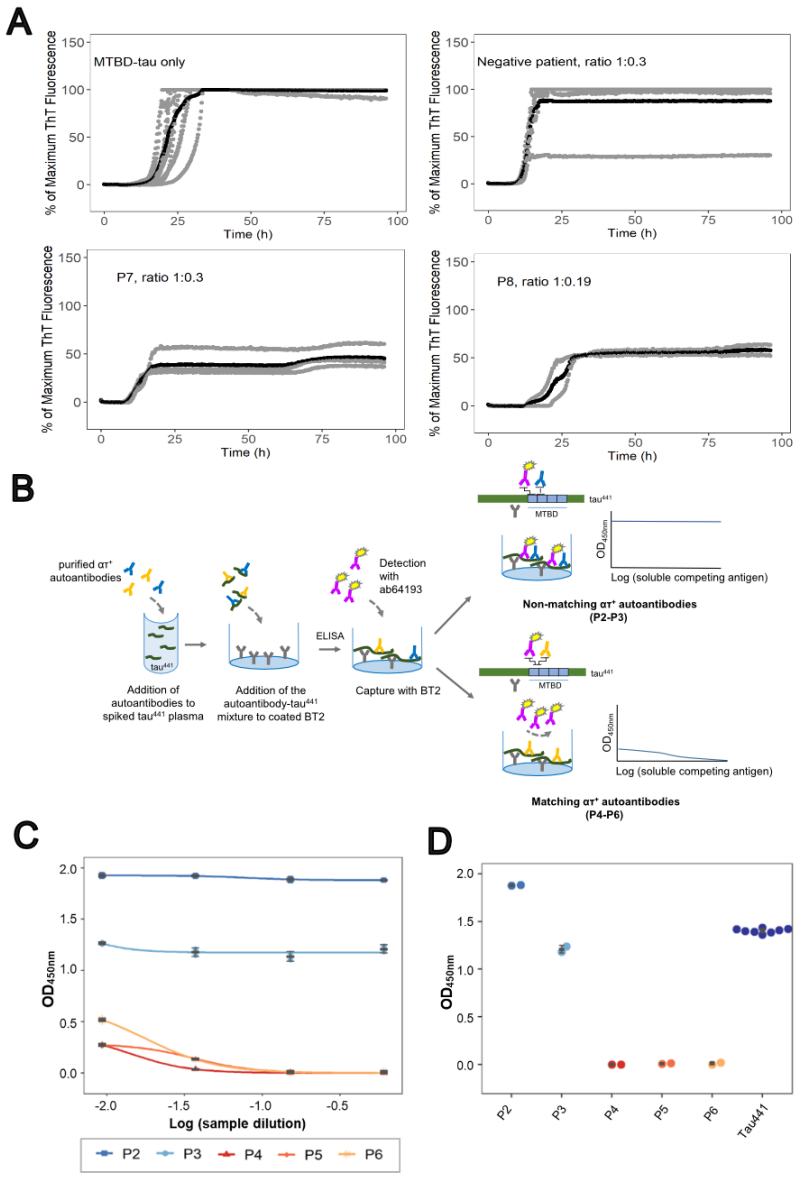

Figure 3. Natural ατ autoantibodies inhibit tau aggregation and impair tau detection. A. Kinetic aggregation curves of MTBD-tau followed by ThT fluorescence in the absence (n=12) or presence of purified ατ autoantibodies (patient P7 (n=4) and P8 (n=2)) or antibodies from an ατ- sample (n=6). Stoichiometric ratios as indicated. Gray lines indicate individual replicates and black lines the average of the replicates. B. Principle of the competition sandwich ELISA. C. Competitive sandwich ELISA to assess the ability of purified anti-tau autoantibodies with matching (P4-P6) and non-matching (P2 and P3) epitopes to the commercial detection antibody, ab64193, to impair

the detection of free tau441 spiked in plasma (dark blue). Serial dilutions of purified anti-tau antibodies are shown in (C) and binding at highest anti-tau antibody concentrations in (D).

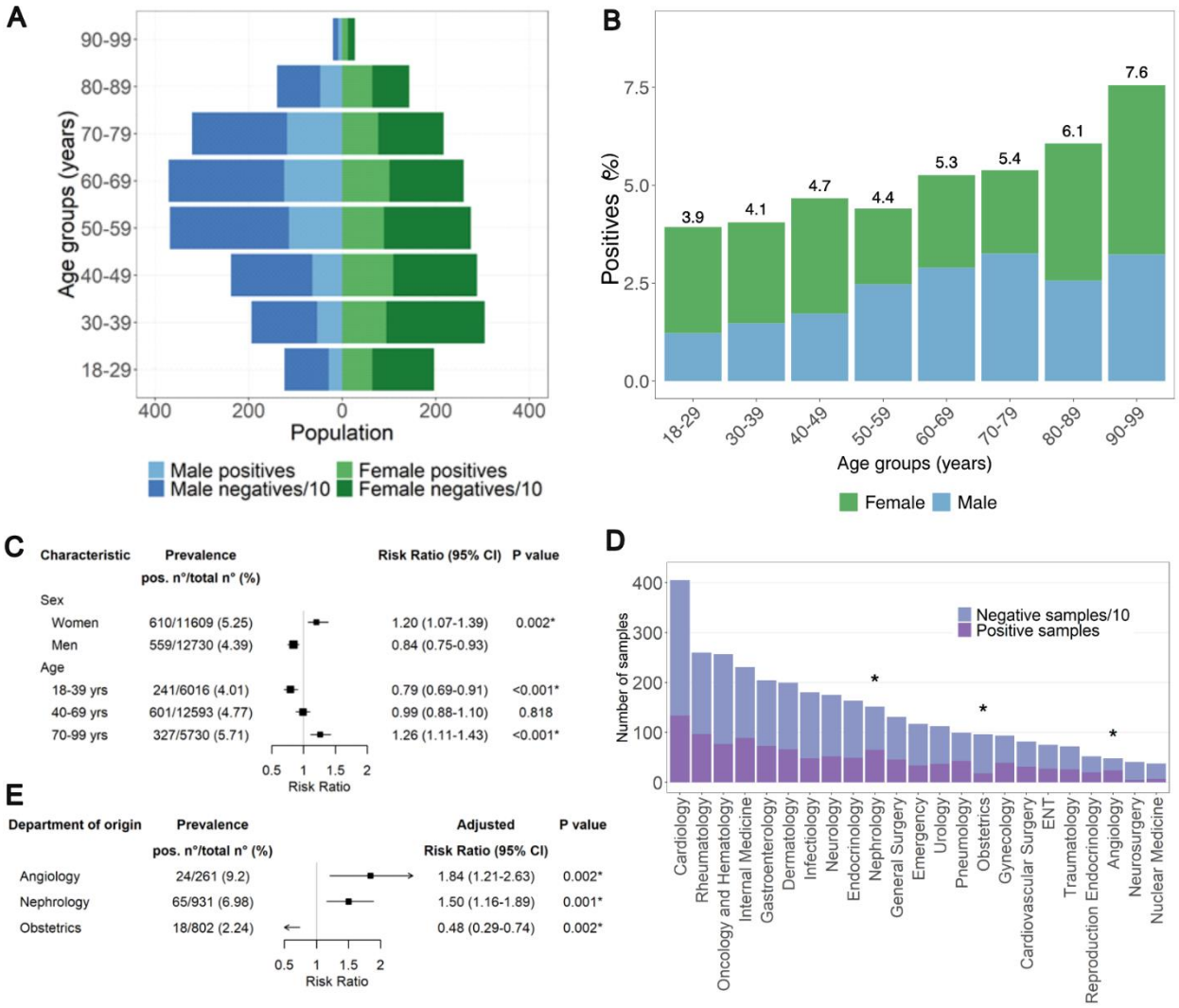

Figure 4. Demographic characteristics of hospital patients' cohort. A. Age and sex pyramid of positive and negative individuals. **B.** Percentage of positives among hospital patients across decadic age groups. The numbers on top of each bar correspond to the positivity rates. χ^2 test for trend in proportions. **C.** RR ± 95% CI for $\alpha\tau^+$ autoantibodies according to sex and age groups. Asterisks: P < 0.05 after Bonferroni correction. **D.** Break-down of samples by clinical department. Asterisks: P < 0.05 (two-proportions z-test with Bonferroni correction). **E.** aRR ± 95% CI for $\alpha\tau^+$ samples by clinical department. Asterisks: P < 0.05 after Bonferroni correction.

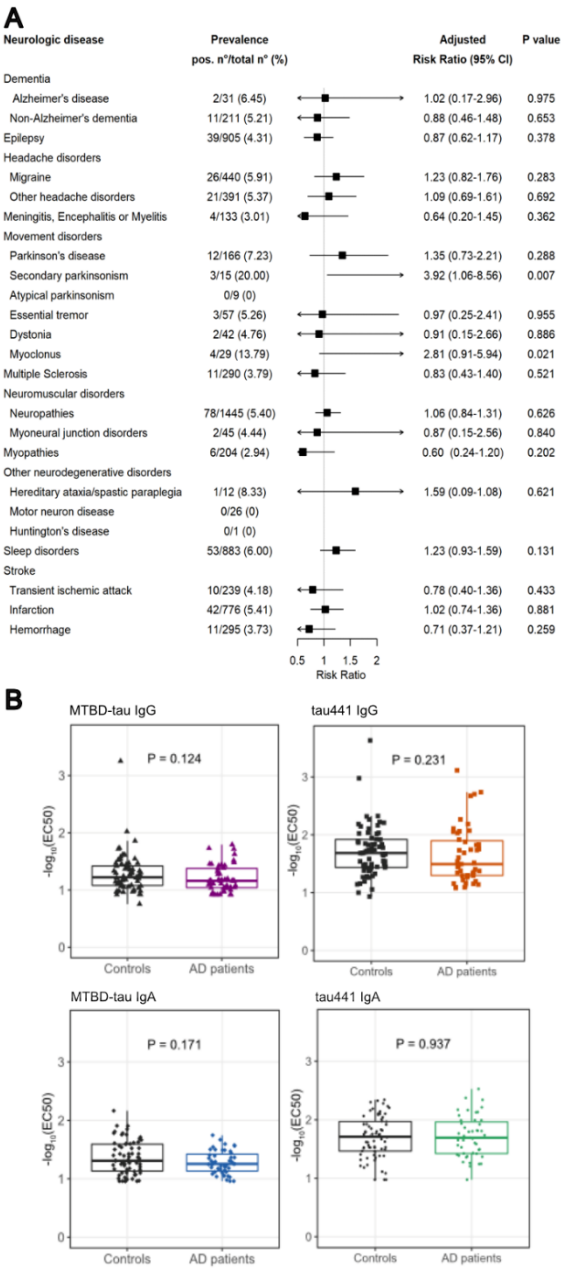

Figure 5. aRR of MTBD-tau-autoreactivity for major groups of neurological disorders and reactivity profiles for AD screen. **A.** aRR and 95% CI (I bars) for $\alpha\tau^{+}$ autoantibodies according to different groups of neurological disorders. No P values remained significant after Bonferroni correction. **B.** Boxplots showing the 25th, 50th (median) and 75th percentiles of the reactivity profiles for AD and control patients (Mann-Whitney U test).

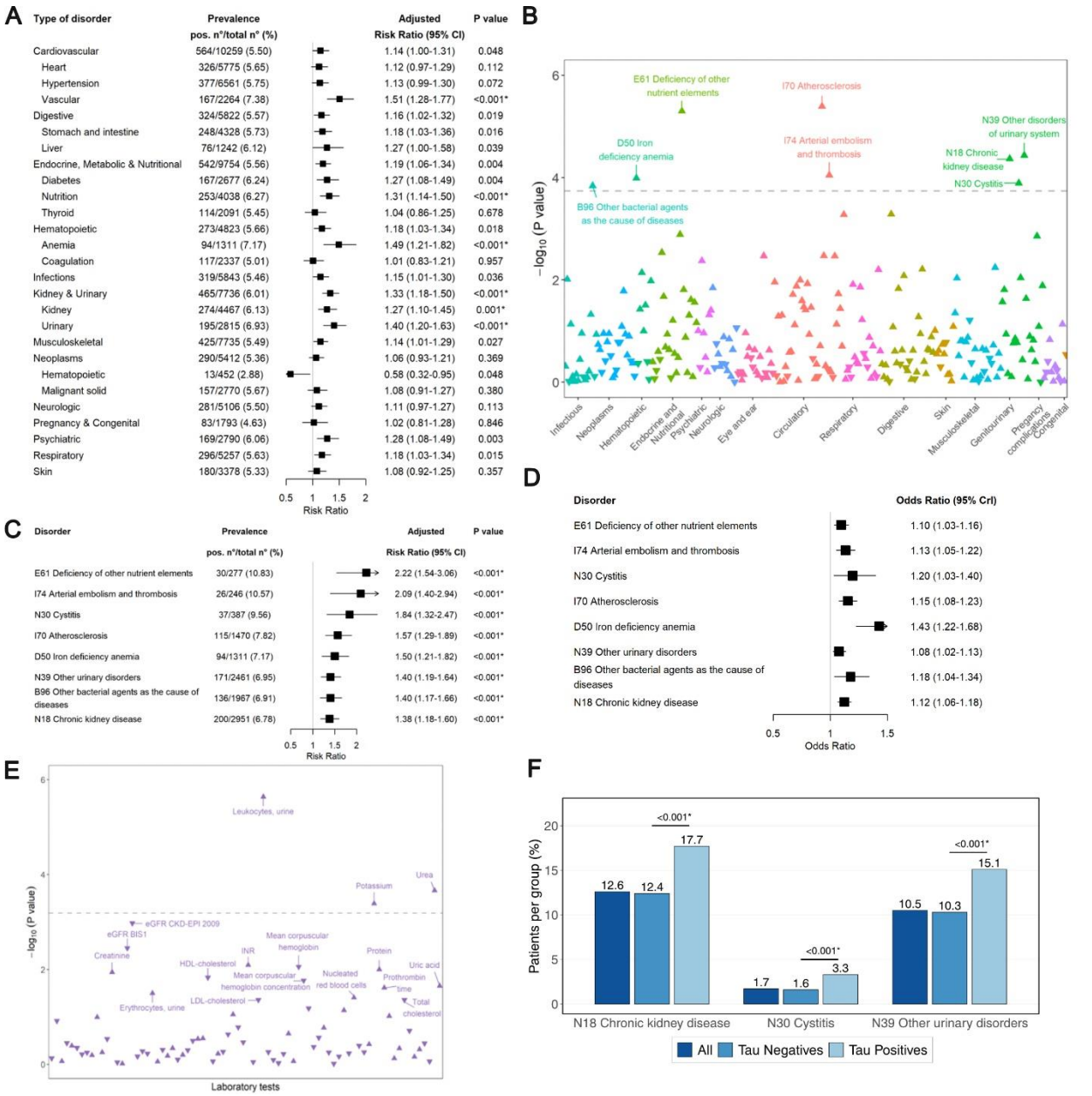

Figure 6. Association of MTBD-tau IgG autoantibodies with systemic disorders and clinical laboratory data. A. aRR ± 95% CI (bars) for $\alpha\tau^+$ autoantibodies grouped 27 different main systemic clinical conditions. Asterisks: $P < 0.05$ after Bonferroni correction. **B.** $-\log_{10}$(P value) of the log-binomial regression for the presence of plasma MTBD-tau IgG autoantibodies for 276 disorders according to ICD-10 codes and adjusted for age and sex. Triangles pointing upwards and downwards: positive and coefficients, respectively; gray dashed line: $P < 0.05$ after Bonferroni correction (here and henceforth). P values significant after Bonferroni adjustment are labelled with the ICD codes. **C.** Same as (A), but according to individual disease entities from (B). **D**. Bayesian

logistic regression adjusted for age and sex on ICD-10 codes significantly associated in B. and using -$\text{logit}_{10}(EC_{50})$ as continuous outcome (odds ratio ± 95% credible intervals). This analysis confirms the positive association of these ICD-10 codes with ατ reactivity (from B). **E.** $\log_{10}$(P value) of the log-binomial regression for the presence of plasma MTBD-tau IgG autoantibodies and clinical laboratory parameters. P values significant after Bonferroni adjustment are labelled with the ICD codes. The gray dashed line indicates the significance level after Bonferroni correction (<0.05/106=0.00047). eGFR CKD-EPI 2009: estimated glomerular filtration rate using the Chronic Kidney Disease Epidemiology Collaboration 2009 equation; eGFR BIS1: estimated glomerular filtration rate using the older adults Berlin Initiative Study 1 equation. INR: international normalized ratio. LDL: low-density lipoprotein. HDL: high-density lipoprotein. **F.** Calculated prevalence of different ICD-10 codes in the total cohort (dark blue), $\alpha\tau^-$ (intermediate blue) and $\alpha\tau^+$ samples (light blue). P-values < 0.001 (two-proportions z-test).